

# On the Correlation Between Kink Effect and Effective Mobility in InAlN/GaN HEMTs

P. Altuntas, N. Defrance, M. Lesecq, A. Agboton,  
R. Ouhachi, E. Okada, C. Gaquiere, J.-C. De Jaeger  
IEMN-CNRS UMR 8520  
Av. Poincare, Cite Scientifique Villeneuve d'Ascq, France  
philippe.altuntas@ed.univ-lille1.fr

E. Frayssinet, Y. Cordier  
CRHEA-CNRS UPR 10  
rue Bernard Gregory, Valbonne, France

**Abstract—** This paper reports on the kink effect observed in InAlN/GaN high electron mobility transistors. Electrical characterizations were carried out to point out the influence of this phenomenon on transistor behaviour. It is demonstrated that the kink effect is directly correlated to shallow traps located under the conduction band. A model is proposed to highlight the influence of scattering effects on the effective mobility, permitting to describe accurately the locus of the so-called kink voltage for a gate bias close to the pinch-off voltage.

**Keywords—**InAlN/GaN; high electron mobility transistor (HEMT); kink effect; effective mobility; traps

## I. INTRODUCTION

In recent years, the high electron mobility transistors (HEMTs) provided promising results in terms of high frequency and high power applications. In particular, the lattice-matched InAlN/GaN heterostructures with thin barriers offer a high charge density compared with conventional AlGaN/GaN heterostructures due to the stronger spontaneous polarization in this material system [1]. Despite these outstanding properties, the HEMT performance remains inherently limited by physical and electrical parasitic phenomena. Among these constraints, kink effect is detrimental to the device performance. Usually, kink effect is characterized by a sudden rise of the output conductance  $g_d$  in the saturation regime and a compression of the transconductance  $g_m$  as well, degrading the transistor performance [2]. Several authors emphasize the direct correlation between impact ionization and trapping effects to explain kink phenomenon. In the case of GaAs MESFETs, Horio *et al* [3] showed that this phenomenon takes origin from the band to band impact ionization and subsequent hole dynamics and recombination. However, for a wider band gap material, kink effect may result from the impact ionization through traps states within the forbidden band gap. As a consequence, kink effect is strongly correlated with trapping and releasing of trapped electrons by hot carriers. Brar *et al.* [4], suggested that kink effect is generated by interband impact ionization in spite of the wide band gap of the GaN channel. Otherwise, Meneghesso *et al.* [5] showed that kink effect could be induced by intraband impact ionization of deep levels within the GaN buffer layer. In this paper, it is shown that kink effect takes origin from impact ionization of shallow levels in the vicinity of the gate. A physical model is proposed involving a single level below the conduction band associated with the concept of the effective electron mobility.

Considering a capture/emission process through one trap level, Shockley-Read-Hall modeling can be applied and directly correlates the capture rate with capture cross section [6]. As a result, a comparison between the measured and modeled kink locus versus gate voltage is proposed, showing a good agreement, especially when the gate voltage becomes closer to pinch-off, for the first time too our knowledge. These results tend to confirm our preliminary assumptions and correlates kink effect and shallow traps through the effective electron mobility.

## II. DEVICE DESIGN AND FABRICATION

InAlN/GaN heterostructure was grown on a high-resistivity silicon (111) substrate by Metal-Organic Chemical Vapor Deposition (MOCVD). The device layer structure consists of a 10 nm thick  $\text{In}_{0.17}\text{Al}_{0.83}\text{N}$  barrier with 1.5 nm thick AlN interlayer used to reduce alloy scattering and to improve carrier confinement within the 2D electron gas (2DEG). The buffer consists of a 1.7  $\mu\text{m}$  thick GaN (Fig. 1). Transistors are fabricated using an electron-beam lithography process and starts with thee Ti/AI/Ni/Au ohmic contact deposited by evaporation followed by a rapid thermal annealing at 850°C for 30s. Transmission Line Modeling data reveal a sheet resistance  $R_{\text{SH}}=346\Omega/\square$  and a contact resistance  $R_{\text{C}}=0.26\Omega\cdot\text{mm}$ . This structure provides a 2DEG with a total charge density  $N_s$  of  $1.3\times 10^{13} \text{ cm}^{-2}$  and an electron mobility of  $1370\text{cm}^2/\text{V.s}$  obtained from Hall measurement. Two fingers gate electrodes are patterned with different gate lengths of  $L_G = 75, 100, 150$  and  $200 \text{ nm}$  for a total gate development of  $50\mu\text{m}$ . The Schottky gate metal consists of evaporated Ni/Au (40/300nm) stack. Devices are passivated with a SiN/SiO<sub>2</sub> bilayer deposited by PECVD at 340°C.

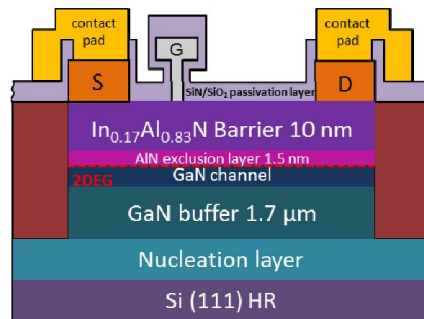


Fig. 1. Cross section of the fabricated InAlN/GaN-on-Si HEMT

### III. DEVICE CHARACTERIZATION

Fig.2 shows the forward I-V characteristics of a device featuring a gate length ( $L_g$ ) of 100nm, a source-to-drain spacing of 2.5 $\mu\text{m}$  and a gate-to-source spacing of 400nm. A maximum saturated drain current of  $1.1\text{A.mm}^{-1}$  is obtained for an applied gate-to-source voltage  $V_{GS}$  of +1V. The associated extrinsic transconductance reaches  $366\text{mS.mm}^{-1}$  for  $V_{DS}=5\text{V}$ . Additionally, a good  $I_{ON}/I_{OFF}$  ratio of  $10^5$  is observed, associated with a pinch-off voltage of -4V, demonstrating that devices do not suffer from drastic buffer leakage.

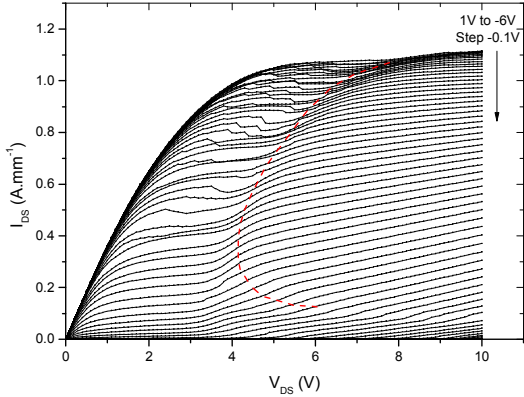


Fig. 2. Forward I-V characteristics of a  $2 \times 25 \times 0.1 \mu\text{m}^2$  HEMT

Kink effect clearly appears on the plotted characteristics. It is emphasized by the dotted red curve. As expected, the locus of kink effect ( $V_{DS,kink}$ ) is strongly dependent on the gate voltage and does not show monotonous evolution. Further characteristics have been obtained using an impedance-meter, where small signal stimuli were used rather than pure DC signals. Fig. 3 represents the small signal drain-to-source conductance ( $g_d$ ) extracted from the real part of the G//C parallel circuit associated with the channel behavior for different AC frequencies ranging from 1 KHz up to 1 MHz. During these measurements, the gate voltage was kept constant at  $V_{GS}=-2.5\text{V}$  and the drain-to-source bias ( $V_{DS}$ ) increased from 2V up to 6V. As a result, kink voltage is, as in DC condition, characterized by a peak in the conductance behavior at around  $V_{DS}=3.7\text{V}$ . This phenomenon also occurred when the AC frequency was swept up to 1MHz, indicating that kink effect is correlated with the presence of shallow traps whose capture/emission rate constant is above 1MHz (i.e. time constant  $< 1 \times 10^6$ s). As an indication, the same measurements were reproduced choosing a gate bias of -1V and the results are plotted in the inset of Fig.3. As expected, kink voltage shifts towards higher  $V_{DS}$  values (the plateau appears around  $V_{DS}=4.5\text{V}$ ). Next section of this paper focuses on the modeling of kink voltage locus depending on the gate-voltage. Many studies were led in different groups to characterize  $V_{kink}$  evolution, but none of these works permits to describe the  $V_{kink}$  shift towards more positive  $V_{DS}$  when the gate bias becomes closer to pinch-off voltage.

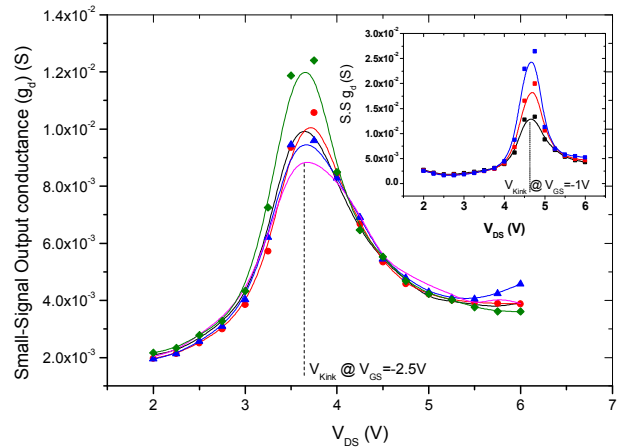


Fig. 3. Measured small-signal channel conductance for AC frequencies sweeping for 1 KHz up to 1 MHz.

### IV. MODELING OF THE TRAPS IONIZATION PROCESS

#### A. Locus of kink effect in the $I(V)$ characteristic

Assuming that kink effect is related to electron filling /release process within shallow traps, it can be assumed that the energy needed for an electron to ionize a trap is [7]:

$$\frac{1}{2}m^*v^2 + k_bT = E_t \quad (1)$$

This total energy  $E_t$  represents the sum of the kinetic and thermal energies of an electron in a 2DEG configuration.  $T$  is the temperature,  $k_b$  the Boltzmann constant,  $m^*$  the effective mass and  $v$  the electron velocity.  $E_t$  refers to the considered trap energy with respect to the bottom of the conduction band. The electron velocity can be related to the effective mobility using the well-known silicon-like relation [8]:

$$\frac{1}{2}m^*\left(\frac{\mu_{eff}\cdot Ek\cdot v_{sat}}{((\mu_{eff}\cdot Ek)^{\beta}+v_{sat}^{\beta})^{1/\beta}}\right)^2 = E_t - k_bT \quad (2)$$

where  $\beta=2$  accounts for the transition factor between the low-field regime and the velocity saturation regime. The effective electron mobility is designed as  $\mu_{eff}$  and  $v_{sat}$  represents the saturation velocity of the electrons in the GaN channel. This relation is satisfied especially when the intrinsic electrical field coincides with the appearance of kink effect. This assumption implies that  $E=E_k$ . A first order modeling can be proposed assuming that  $E_k = V_{dsi,K}/L_{g,eff}$ . Eq.(2) becomes:

$$\frac{1}{2}m^*\left(\frac{\mu_{eff}\cdot V_{dsi,K}/L_{g,eff}\cdot v_{sat}}{((\mu_{eff}\cdot V_{dsi,K}/L_{g,eff})^{\beta}+v_{sat}^{\beta})^{1/\beta}}\right)^2 = E_t - k_bT \quad (3)$$

In eq. (3),  $V_{dsi,K}$  is the intrinsic drain to source voltage where kink effect occurs and  $L_{g,eff}$  related to the effective gate length. Solving for  $V_{dsi,K}$  gives:

$$V_{dsi,K} = \frac{L_{g,eff}\cdot v_{sat}}{\mu_{eff}} \sqrt{\frac{E_t - k_bT}{\frac{1}{2}m^*v_{sat}^2 - (E_t - k_bT)}} \quad (4)$$

In these conditions, the locus of kink voltage with respect to the applied gate bias should be correlated with the effective mobility whose value is affected by both the surface scattering phenomenon and the vertical electrical field in the vicinity of the gate contact. As a consequence, a special attention has to be paid on the extraction of the effective mobility with respect to the gate-to-source voltage. This work is described in the next section of this paper.

### B. On the accurate extraction of the effective mobility

A HEMT device featuring an effective gate length  $L_{g,eff}$  and a width  $W$  is considered. The drain current  $I_{DS}$  is written as a combination of drift and diffusion currents [6]:

$$I_{ds} = \frac{W \cdot Q_n \cdot \mu_{eff} \cdot V_{DS}}{L_{g,eff}} - W \cdot \mu_{eff} \cdot \frac{kT}{q} \frac{\partial Q_n}{\partial x} \quad (5)$$

where  $Q_n$  is the mobile sheet charge density, and  $\mu_{eff}$  the effective mobility. When measurements are performed at sufficiently low  $V_{DS}$ , the channel charge is more uniform from source to drain, allowing the diffusive second term to be neglected. Solving for the effective mobility  $\mu_{eff}$  and writing  $g_d = I_{ds}/V_{DS}$  gives:

$$\mu_{eff} = \frac{g_d \cdot L_{g,eff}}{W \cdot Q_n} \quad (6)$$

The dependence of the effective mobility versus the gate voltage is considered through the induced variation of the mobile sheet charge density  $Q_n(V_{gs})$ . The linear model usually implemented to characterize the charge modulation suffers from a restricted validity within the so-called strong inversion regime. Thus, a more adequate modeling of  $Q_n(V_{gs})$  is needed so that the effective mobility can be extracted whatever the considered gate-to-source voltage. Consequently, several improvements were brought to the classical procedure to get accurate values of  $\mu_{eff}$ .

#### 1) Effect of series resistance

As the intrinsic source-to-drain voltage depends on both the current and the series resistance, the effective mobility must consider the intrinsic conductance [9]. This is given through eq. (7):

$$g_d = \frac{g_{d,m}}{1 + (R_s + R_d)g_{d,m}} \quad (7)$$

where  $g_{d,m}$  represents the measured output conductance at low bias (typically 100mV),  $R_s$  and  $R_d$  account for the effect of the source and drain resistances respectively. These last are commonly quantified knowing the contact and sheet resistances values:

$$R_{s,d} = \frac{R_c}{W} + \frac{L_{gs,gd} \times R_{sheet}}{W} \quad (8)$$

Applied to our topology, it gives  $(R_s + R_d) = 1.42 \Omega \cdot \text{mm}$ .

#### 2) Accurate modeling of the sheet charge density $Q_n$

As exposed previously, an adequate modeling of the sheet charge density is needed to unambiguously extract the effective mobility in low, moderate and strong inversion regimes. In this frame, a simplified expression of the virtual

source model (VSM) is used to describe the influence of the gate voltage on the 2DEG density [10]. This model relies on the expression of  $Q_n$  as described in eq. (9).

$$Q_n = \frac{\epsilon_{InAlN}}{t_{InAlN}} \cdot \eta \varphi_t \cdot \ln \left( 1 + \exp \left( \frac{V_{gs} - V_{th}}{\eta \varphi_t} \right) \right) \quad (9)$$

where  $\epsilon_{InAlN}$  and  $t_{InAlN}$  are the dielectric constant and the gate to channel thickness respectively,  $\varphi_t$  refers to the thermal voltage,  $V_{th}$  is the threshold gate-to-source bias and  $\eta = \frac{s}{\varphi_t \ln(10)}$ ,  $S$  accounting for the sub-threshold slope. The values that were used to describe  $Q_n$  evolution with the gate voltage are summarized in the next table.

TABLE I. Parameters used within the simplified VSM

$\epsilon_{InAlN}$ (F.m <sup>-1</sup> )	$t_{InAlN}$ (nm)	$S$ (V/V)	$V_{th}$ (V)	$\varphi_t$ (eV)
$9.1 \cdot 10^{-11}$	13.5	0.15	-4	0.025

The comparison with results derived from Schrödinger-Poisson self-consistent simulation gives good agreement, characterized by a correlation factor close to 0.97 for gate bias ranges in moderate and strong inversion regimes. Additionally, this model permits to implement the subthreshold behavior of the charge modulation through the  $S$  parameter directly measured on the device under test.

#### 3) Impact on the effective mobility extraction

The effective mobility as a function of the gate-to-source voltage is plotted in fig.4. As expected, an important underestimation is operated when the “as-measured” conductance is used; this is critically improved when the series resistances accounting for source-to-gate and gate-to-drain regions are taken into account. In the same way, the evolution of  $\mu_{eff}$  close to and slightly beyond threshold can be trusted in a more significant way since the used  $Q_n$  modeling permits to get accurate charge modulation description in these working conditions.

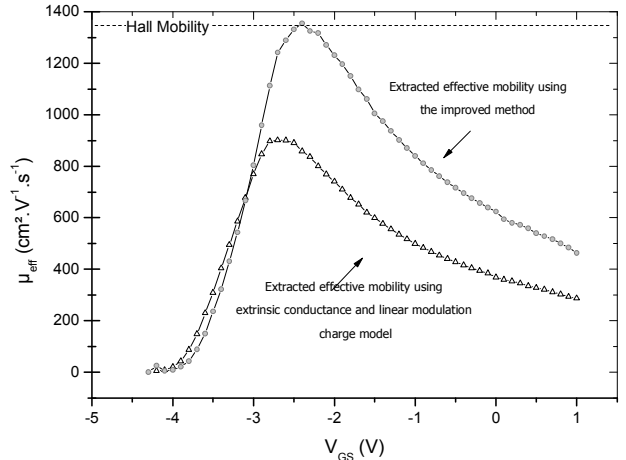


Fig. 4: Measured effective mobility using usual and improved extractions

The fact that  $\mu_{eff}$  peak value closely coincides with the Hall mobility indicates that the electron transport mechanism occurs within a well-confined 2DEG featuring a high mobility.

For gate voltages moving closer to pinch-off voltage, the carrier confinement is lost and electron may spill into the GaN buffer where the mobility is lower than in 2-dimension configuration [11]. Additionally, a higher electrical field in the vicinity of the gate contact enhances the scattering mechanisms emerging from dislocations and ionized impurities especially when the 2DEG density becomes lower.

## V. RESULTS AND DISCUSSION

The locus of both intrinsic measured and modeled kink voltages versus the considered gate bias is plotted in fig. 5. The best fit is obtained using eq.(4) associated with fitting values of  $v_{sat}=1.1 \cdot 10^5 \text{ m.s}^{-1}$ ,  $m^*=0.2m_0$ ,  $L_{g,eff}=120\text{nm}$  and  $E_t=60.1\text{meV}$ . It must be underlined that all of these parameters are characterized by values close to the physical prediction or in agreement with formerly reported values.

For the first time to our knowledge, the rise of the kink voltage for gate bias close to pinch-off is well reproduced, as well as the linear behavior in the so-called strong inversion regime. This observation permits to validate our preliminary assumptions. Additionally, the order of magnitude referring to  $V_{kink}$  values are in good agreement with those experimentally obtained. As it was expected in the previous section, kink effect is engendered by the presence of shallow traps, since the fitted value of  $E_c-E_t$  is only 60meV. The Shockley-Read-Hall emission-recombination model through one level can be used to extract the effective cross-section [6]. It gives:

$$\sigma_n = \left( v_{th} \tau N_c e^{-\frac{E_t}{k_B T}} \right)^{-1} \quad (10)$$

where  $\sigma_n$  is the effective capture cross-section,  $\tau$  the time constant associated with capture phenomenon,  $N_c$  the density of states in the GaN material,  $T$  the temperature and  $v_{th}$  the thermal velocity of electrons. Using a time constant  $\tau$  smaller than  $1 \cdot 10^{-7} \text{ s}$ , the effective capture cross-section  $\sigma_n$  is found to be above  $2.3 \times 10^{-16} \text{ cm}^2$ . The extracted value of  $E_t$  is consistent with defects already attributed to nitrogen vacancies [12]; further analysis using deep level transient spectroscopy (DLTS) should permit to resolve any ambiguity about the accurate level position and its physical origins.

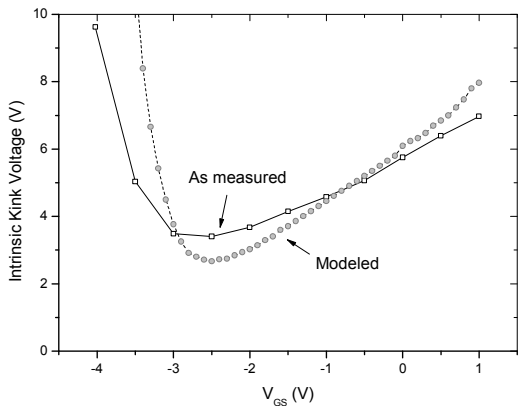


Fig. 5: Locus of the intrinsic kink voltage versus the applied gate bias.

## VI. CONCLUSION

In this paper, static and low-frequency small signal measurements were carried out to characterize kink effect phenomenon in InAlN/GaN devices. It is assumed that this effect takes origin from capture/ionization of electrons through shallow traps in the vicinity of the gate contact. Through scattering phenomenon, these defects directly impact the electrons effective mobility and then they affect the carrier velocity and energy. A simple model was derived permitting to reproduce accurately the kink voltage locus throughout the forward I(V) characteristics of the device. The best fit between measured and modeled data reveals an energy level of 60meV below the conduction band, associated with a capture cross section above  $2.3 \times 10^{-16} \text{ cm}^2$ . For the first time to our knowledge, a complete description of the kink voltage is proposed and correlates the impact of shallow traps with the measured effective mobility.

## ACKNOWLEDGMENT

The authors would like to thank the RENATECH technological network, the French National Research Agency for its financial support in the frame of SATELLITE contract and the cluster of excellence GANEX (ANR-11-LABX-0014).

## REFERENCES

- [1] O. Ambacher, R. Dimitrov et al., "Role of Spontaneous and Piezoelectric Polarization Induced Effects in Group-III Nitride Based Heterostructures and Devices," Phys. stat. Sol.(b) 216, pp. 381-389, 1999.
- [2] S.D. Nsele, L. Escotte et al, "Broadband Frequency Dispersion Small-Signal Modeling of the Output Conductance and Transconductance in AlInN/GaN HEMTs," IEEE Transactions on Electron Devices, vol. 60, no. 4, pp. 1372-1378, 2013.
- [3] K.Horio and A.Wakabayashi, "Numerical Analysis of Surface-State Effects on Kink Phenomena of GaAs MESFETs," IEEE Transactions on Electron Devices, Vol. 47, no. 12, pp 2270-2276, 2000.
- [4] B. Brar, K. Boutros et al., "Impact ionization in high performance AlGaN/GaN HEMTs," High Performance Devices, 2002. Proceedings. IEEE Lester Eastman Conference, pp. 487-491, 2002.
- [5] G. Meneghesso, F. Zanon, M.J. Uren and E. Zanoni, "Anomalous Kink Effect in GaN High Electron Mobility Transistors," Electron Device Letter, Vol. 30, no. 2, pp. 100-108, 2009.
- [6] D.K. Schroder, "Semiconductor Material and Device Characterization", Third Edition, Published by John Wiley & Sons, Inc., Hoboken, New Jersey, 2006.
- [7] M. Sarajlic, R. Ramovic, "On the relationship between effective electron mobility and Kink effect for short-channel PD-SOI NMOS devices, Int. Journal of Mod. Physics B, Vol.22, no 16, 2008
- [8] D.M. Caughey, and R.E. Thomas, "Carrier Mobilities in Silicon Empirically Related to Doping and Field", Proceedings of the IEEE, vol. 55, no. 12, pages 2192-2193, 1967.
- [9] S.Y. Chou, D.A. Antoniadis, "Relationship between measured and intrinsic transconductance of FET's", IEEE Transactions on Electron Devices, vol. 34, no. 2, pp. 448-450, 1987.
- [10] U. Radhakrishna, L. Wei, D.S. Lee, T. Palacios, D. Antoniadis, "Physics-based GaN HEMT Transport and Charge Model: Experimental Verification and Performance Projection". Electron Devices Meeting (IEDM), Proc. of, 2012
- [11] M. A. Negara, D. Vekslar, et al., "Analysis of effective mobility and hall effect mobility in high-k based In0.75Ga0.25As metal-oxide-semiconductor high-electron-mobility transistors", Applied Physics Letters 99, 232101 (2011)
- [12] M. Levenshtein, S. Rumyantsev, M. Shur, "Properties of advanced semiconductor materials: GaN, AlN, InN, BN, SiC, SiGe", Wiley, 2001